A LIFE PREDICTION MODEL FOR CREEP-FATIGUE INTERACTION

A. Martín Meizoso, J.M. Martínez Esnaola, J.Mª Rodríguez Ibabe and M. Fuentes Pérez

A simple model for crack initiation under creep-fatigue conditions is proposed. The model is based on the identification of the active deformation mechanisms of the material for a given loading condition. Each deformation mechanism is assumed to be described by an independent damage equation of the Coffin-Manson type. A simple summation rule is proposed to account for the total damage. Results obtained for AISI 316L stainless steel under creep-fatigue conditions show a good correlation with the measured data and the failure modes predicted by the model agree with those observed in the experiments.

INTRODUCTION

A number of methods based on rather empirical criteria have been proposed for life assessment under creep-fatigue conditions. Most of them consist of assuming that the variables involved in the experiments (typically the stress or strain range and the number of cycles to failure) are related through a given relationship which depends on a number of unknown parameters. While these approaches are useful to correlate data from the experiments, there is the experimental evidence that the lack of well established physical basis of the behaviour of the material makes it difficult to extend the results outside the range covered by the experiments.

The model presented in this paper is based on Ashby's deformation mechanism maps of the material (1). As proposed by Ashby, under conditions of monotonic loading, crystalline solids can experience plastic deformation according to a number of alternative mechanisms. Hence, the total strain rate at a given instant can be calculated from the contributions of each active mechanism. Using this approach, the total strain range can be partitioned into the strain ranges corresponding to each deformation mechanism involved in the stress-temperature cycle. A simple summation rule is proposed to account for the total damage. The model allows to explain the different failure modes observed in the experiments.

Centro de Estudios e Investigaciones Técnicas de Guipúzcoa (CEIT), Pº Manuel de Lardizábal, 15, 20009 San Sebastián, Spain

Once the different damage mechanisms have been characterised, the proposed life prediction method could be extended to longer times (outside the range covered by the experimental data) provided that one can ensure that no new damage mechanism will appear.

DESCRIPTION OF THE MODEL

The inability of phenomenological models to assess creep-fatigue interaction outside the range covered by the experiments has been always attached to differences in the deformation mechanisms involved in the process. What is proposed here is to face the problem directly from a micromechanistic point of view. The model is based on the following assumptions:

i) Each independent deformation micromechanism has its own failure equation.

ii) The second assumption is the form of these failure equations. As a first approximation, a Cofin-Manson relationship is proposed for each micromechanism.

$$D_i = \frac{\Delta\varepsilon_i}{\Delta\varepsilon_{ic}} N^{\alpha_i} \qquad (1)$$

where D_i stands for the damage produced by the i-deformation micromechanism, $\Delta\varepsilon_i$ is the deformation produced by the i-mechanisms, and $\Delta\varepsilon_{ic}$ and α_i are related to the micromechanism ductility and damage irreversibility, respectively. This type of equation has been proved to work well for pure fatigue where dislocation movement is the main deformation micromechanism. What is assumed here is that this equation holds true for all the deformation micromechanisms.

iii) Finally, some assumption should be made about how different micromechanisms cooperate for failure. The simplest hypothesis is to consider that damages produced by different micromechanisms cumulate for failure:

$$D = \sum_{i=1}^{m} D_i \qquad (2)$$

where m stands for the number of operative micromechanisms.

In order to determine the damage produced by each micromechanism it is required to estimate the deformation due to each particular micromechanism. To this purpose, Ashby's deformation mechanism maps may be used. The deformation produced by the i-mechanism may be computed integrating, along the cycles, Ashby's strain rate equations:

$$\Delta\varepsilon_i = \int \dot{\varepsilon}_i(\sigma,T)\, dt \qquad (3)$$

Obviously, equations for the strain rates are merely approximative (note also that equations fit monotonic deformation and not cyclic conditions) and should be used to partition the actual inelastic strain into different micromechanisms.

In order to compute the constants for each micromechanism in the damage equations ($\Delta\varepsilon_{icrit}$, α_i), experiments where failures were due to each particular micromechanism should be used. Also note that constants in equation (1) should be measured for the service temperature range.

The applicability of the damage equations can be assessed through the fracture modes observed in the experiments. It is possible to compute D_i at failure for different micromechanisms and these should be reflected on fracture surfaces.

RESULTS ON AISI 316L STAINLESS STEEL

The model described in the previous section has been used to model AISI 316L stainless steel under isothermal low cycle fatigue conditions. The experimental arrangement and results can be found elsewhere (2-5). Fig. 1 shows the deformation mechanisms for AISI 316L at 625ºC and grain size, d=50 μm. At 625ºC, two damage mechanisms were identified: dislocation damage and grain boundary sliding damage.

Cyclic fatigue tests were conduced under diametral strain control in the range 0.14%-1.27%. A symmetric triangular wave shape was used with axial strain rates in the range 0.9×10^{-3} - $7.6\times10^{-3}\ s^{-1}$. Fig. 2 shows the results obtained for pure fatigue (open circles). In the figure, $N_{5\%}$ represents the number of cycles corresponding to 5% of load reduction. The estimated damage equation for dislocation induced failure is given by

$$D_{\text{dislo}} = \frac{\Delta\varepsilon\ \text{dislo}}{0.531}\, N^{0.581} \qquad (4)$$

Additional tests were conducted with hold times at the maximum stress between 1 min and 1h (see Fig.2). The axial strain rate corresponding to the loading and unloading parts of the cycle was $4\times10^{-3}s^{-1}$. In order to apply equation

(1) it is necessary to estimate the strain range due to each deformation mechanism. This can be achieved by integrating the strain rates as described in equation (3). A more classical approach consists of assigning the strain to the different mechanisms according to the strain rate at each point in the cycle. This requires the definition of a transition strain rate which should be chosen so as to produce the same damage rate in both mechanisms. This in turn requires the knowledge of the damage equation for each mechanism. Any iterative procedure may be used to solve this problem. In particular the transition strain range to change from dislocation damage to grain boundary sliding damage in the conditions of the present investigation was estimated to be $5x10^{-5}s^{-1}$.

According to this estimation, the strain produced during the hold time above the critical strain rate was assigned to dislocation mechanisms ($\Delta\varepsilon_{dislo}$) and the strain produced at strains rates lower than the critical value was computed as grain boundary sliding strain ($\Delta\varepsilon_{gbs}$). Using the results shown in Fig.2, the equation describing the total damage was found to be

$$D = \frac{\Delta\varepsilon_{dislo}}{0.531} N^{0.581} + \frac{\Delta\varepsilon_{gbs}}{0.064} N^{0.794} \qquad (5)$$

Fig. 3 shows dislocation (fatigue) damage versus grain boundary damage from the experimental results and according to equation (5). The dashed lines represent a factor of two in the number of cycles to failure. It should be noted that only the experimental results where grain boundary damage was larger than dislocation damage were used to fit grain boundary damage equation. Fig. 4 shows the comparison between the observed lives and the predictions obtained using equation (5). Note also that the scatter in Figs. 3 and 4 is comparable with that of pure fatigue results.

CONCLUSIONS

A micromechanistic model has been presented to account for crack initiation under creep-fatigue conditions. The starting point is the identification of the deformation mechanisms contributing to the total deformation of the material. While this is based on solid physical foundations, some assumptions have been made on the damage equations of the different mechanisms and the way of cooperating to failure.

The present approach has been applied to model isothermal creep-fatigue interaction in AISI 316L stainless steel. The results obtained show a good correlation with the measured data and the failure modes predicted by the model agree with those observed in the experiments.

The applicability of the model under thermomechanical loading conditions requires further work and will be investigated in the future. It is envisaged that some parameters involved in the model will become temperature dependent so that experiments should be designed to elucidate this dependence. However the micromechanistic basis of the proposed model suggests that the above method can be applied under non-isothermal conditions provided that the active damage mechanisms are identified.

REFERENCES

(1) Frost, H.J. and Ashby, M.F., "Deformation-mechanism maps", Pergamon Press, Oxford, 1982.

(2) Simón García, S., Rodríguez Ibabe, J.M. and Fuentes Pérez, M., Anales de Mecánica de la Fractura,4, 1987, pp. 95-106.

(3) Simón García, S. and Fuentes Pérez, M., Revista de Metalurgia, 25, 1987, pp. 326-334.

(4) Simón García, S., Rodríguez Ibabe, J.M., Fuentes Pérez, M., Anales de Mecánica de la Fractura, 6, 1989, pp. 133-138.

(5) Martín Meizoso, A., Rodríguez Ibabe, J.M. and Fuentes Pérez, M., "A micromechanistic approach to life assessment under fatigue-creep conditions on AISI 316L stainless steel", to be published.

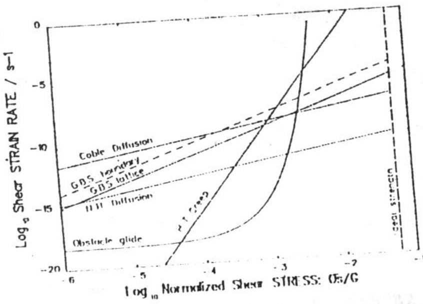

Figure.1 Deformation mechanisms of AISI 316L at 625ºC (d=50μm)

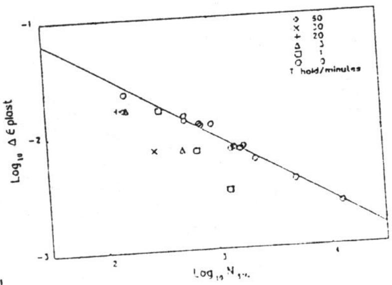

Figure.2 Experimental results for pure fatigue and creep-fatigue in AISI 316L at 625ºC

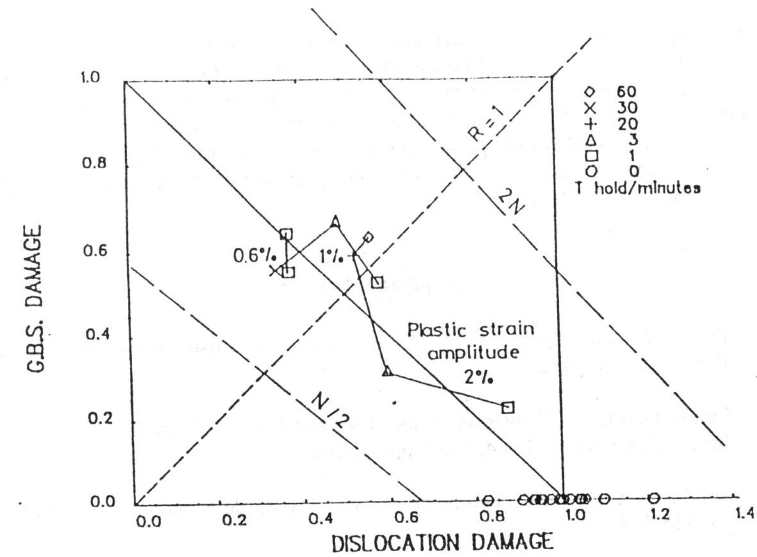

Figure.3 Dislocation damage versus grain boundary damage for AISI 316L at 625ºC.

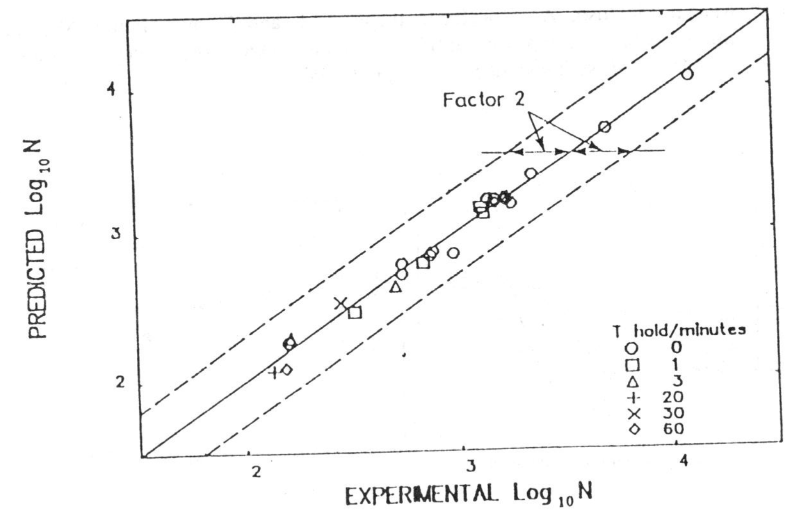

Figure.4 Predicted versus measured number of cycles to failure for AISI 316L at 625ºC.